AIAA JOURNAL
Vol. 31, No. 10, October 1993

Three-Dimensional Shock-Wave/Boundary-Layer Interactions with Bleed

T. I-P. Shih* and M. J. Rimlinger†
Carnegie Mellon University, Pittsburgh, Pennsylvania 15213
and
W. J. Chyu‡
NASA Ames Research Center, Moffett Field, California 94035

Computations were performed to investigate the physics of three-dimensional, shock-wave/boundary-layer interactions on a flat plate in which fluid in the boundary layer was bled through a circular hole into a plenum to control shock-wave induced flow separation. This study revealed two underlying mechanisms by which bleed holes can control shock-wave/boundary-layer interactions. It also showed how bleed-hole placement relative to where the incident shock wave impinges affects upstream, spanwise, and downstream influence lengths. This study is based on the ensemble-averaged, full compressible Navier-Stokes equations closed by the Baldwin-Lomax turbulence model. Solutions to these equations were obtained by an implicit, partially split, two-factored method with flux-vector splitting on a chimera overlapping grid.

Introduction

SHOCK-WAVE/boundary-layer interactions and their control play an important role in many applications (e.g., turbojet inlets, wind tunnels, and airframes of supersonic aircraft). This is because shock waves can induce boundary-layer separations which in turn can lead to highly undesirable consequences (e.g., it can cause the unstart condition in a turbojet inlet). One effective way of controlling shock-wave induced flow separation is to place bleed holes near where the shock wave strikes the boundary layer. The ability of bleed holes to prevent separation for subsonic flows is well understood. For subsonic flows, bleed holes remove air near the wall surface where the momentum is low so that the remaining high-momentum air can withstand adverse pressure gradients without separating. For supersonic flows with shock waves, the mechanism is more complex and has not been well understood.

The importance of bleed holes for controlling shock-wave/boundary-layer interactions has led a number of investigators to use both experimental and numerical methods to study this problem (see reviews by Delery[1] and Hamed and Shang[2]). According to Hamed and Shang,[2] although all experimental studies agree that bleed can control shock-wave induced flow separation, there are disagreements on how the bleed-hole size and location affect the bleed process. These discrepancies indicate the complexities of the flow in the region about bleed holes. In that region, many geometric and operating parameters can affect the physics of the flow with different parameters dominating under different conditions.

Hamed and Lehnig[3,4] and Hahn et al.[5] performed two-dimensional numerical studies to address the discrepancies in the experimental data. In these studies, bleed holes are modeled as slots. Hamed and Lehnig studied shock-wave/boundary-layer interactions over a flat plate with a single bleed hole in which the depth of the hole is three times its width, and the flow through the bleed hole is always choked. Under the conditions of their study, they showed that placing a bleed hole just beneath where the shock wave strikes the boundary layer is the most effective in eliminating flow separation. Hahn et al. studied shock-wave/boundary-layer interactions over a flat plate with one or two bleed holes that were connected to a plenum in which the flow may or may not be choked within the bleed hole or holes. Their study showed the details of the flowfield around bleed holes including how the plenum affects the bleed process. They also showed the effects of the following parameters in controlling shock-wave induced flow separation: location of bleed hole or holes in relation to where the incident shock impinged on the boundary layer, size of bleed holes in relation to boundary-layer thickness, number of bleed holes, spacing between bleed holes, and depth-width ratio of bleed holes.

Although the aforementioned studies give valuable insights into the physics of shock-wave/boundary-layer interactions with bleed, realistic bleed holes are three dimensional instead of two dimensional. To date, no one has reported an experimental or a numerical study that showed the details of three-dimensional, shock-wave/boundary-layer interactions with bleed. The objective of this investigation is to study numerically the physics of three-dimensional, oblique shock-wave/boundary-layer interactions on a flat plate fitted with a single circular bleed hole that is connected to a plenum. More specifically, that objective is as follows. First, identify the mechanism or mechanisms by which a bleed hole affects the response of a boundary layer to an incident oblique shock wave. Second, study how the location of a bleed hole in relation to where an incident shock wave impinges on the boundary layer affects upstream, spanwise, and downstream influence lengths. In this numerical study, the flowfield was calculated not only above the plate and in the bleed hole but also in the plenum.

Since realistic problems involving shock-wave/boundary-layer interactions with bleed are often very complex, with multiple bleed holes and a wide range of operating conditions, this study represents one of many that must be done in order to understand the physics of such flows. The approach taken here is to understand first what happens at one hole for a simple geometry with a well-understood incident shock wave and a well-defined boundary-layer profile before trying to understand what happens at multiple holes with complex shock structures (many shock reflections) before reaching the bleed zone.

Description of Problem

A schematic diagram of the bleed-hole problem studied is shown in Fig. 1. The domain of this problem is the region bounded by the dashed lines, which includes the plenum, the region above the flat plate, and the bleed hole. In this study, the width W of the domain was 0.0762 m (3 in.). The length L and height H of the region above the flat plate were 0.1778 m (7 in.) and 0.0762 m (3 in.), respectively. The plenum had a length L_{P1} of 0.142875 m

Received July 17, 1992; revision received Jan. 8, 1993; accepted for publication March 9, 1993.

*Professor, Department of Mechanical Engineering. Member AIAA.
†Graduate Student, Department of Mechanical Engineering.
‡Research Scientist, Applied Aerodynamics Branch. Member AIAA.

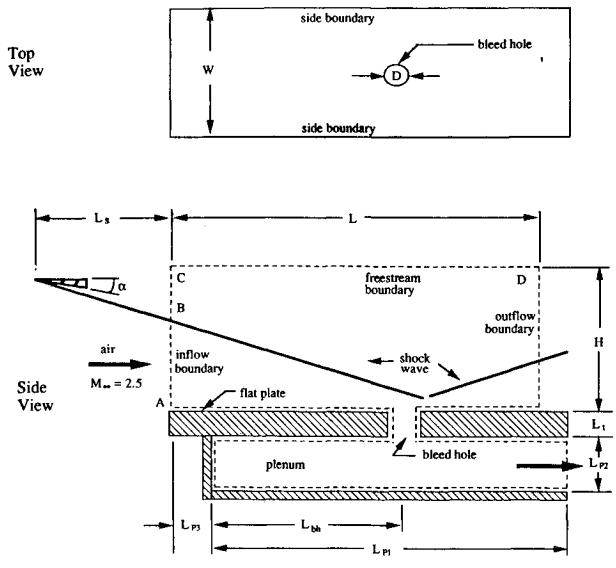

Fig. 1 Schematic diagram of problem studied.

(5.625 in.) and a height L_{P2} of 0.0254 m (1 in.). The distance between the inflow boundary and the left wall of the plenum L_{P3} was 0.06350 m (2.5 in.). Three different bleed hole locations were investigated. For these three locations, the distances between the center of the bleed hole and the left wall of the plenum L_{bh} were 0.0396875 m (1.5625 in.), 0.0428625 m (1.5625+1/8 in.), and 0.0365125 m (1.5625 − 1/8 in.). In all cases, the diameter D and depth L_t of the bleed hole were 0.003175 m (1/8 in.) and 0.0015875 m (1/16 in.), respectively.

For this problem, the fluid that entered the domain was air with a constant specific-heat ratio γ of 1.4. The freestream Mach number M_∞, static temperature T_∞, and density ρ_∞ were 2.5, 134 K, and 0.262 kg/m^3, respectively. This supersonic flow had a turbulent boundary layer next to the flat plate. At the inflow boundary, the thickness of that boundary layer δ was 0.003175 m (1/8 in.), which is equal to the diameter of the bleed hole. To induce flow of air through the bleed hole, the back pressure P_b at the exit of the plenum was set at $0.3P_\infty$, where P_∞ is the freestream static pressure which can be calculated from the freestream temperature and density.

A shock-wave generator characterized by L_s and α caused an oblique shock wave to strike the turbulent boundary layer next to the flat plate. The parameter α was set equal to 7.0 deg, which produced a shock wave that was strong enough to induce flow separation on the flat plate in the absence of bleed. The parameter L_s controls where the shock wave strikes the boundary layer. Here, L_s was chosen so that the shock wave would impinge on the flat plate at L_{bh} equal to 0.0396875 m (1.5625 in.) under inviscid conditions (i.e., if the boundary layer was not present). This location corresponds to the center of one of the three bleed-hole locations investigated and is 0.003175 m (1/8 in.) either before or after the center of the other two bleed-hole locations investigated.

Formulation of Problem

The flow problem described in the preceding section was modeled by the unsteady form of the density-weighted, ensemble-averaged conservation equations of mass, momentum ("full compressible" Navier-Stokes), and total energy written in generalized coordinates and cast in strong conservation-law form. The effects of turbulence were modeled by the Baldwin-Lomax algebraic turbulence model.[6] This simple model was used because more sophisticated k-ϵ models have not been demonstrated to give better results for this type of flow, especially in the region about the bleed hole. A laminar flow was not assumed because the separation region induced by the incident shock wave would be much larger than the one under turbulent conditions so that unrealistically large bleed holes and/or bleed rates would be needed to control flow separation. In this study, the uncertainties associated with the turbulence model were handled by ensuring that all conclusions reached in the results section would not be affected by the turbulence model used.

To obtain solutions to the conservation equations, boundary and initial conditions are needed. The boundary conditions (BCs) employed in this study for the different boundaries shown in Fig. 1 were as follows. At the inflow boundary where the flow is supersonic everywhere except for a very small region next to the flat plate, two types of BCs were imposed. Along segment A-B, all flow variables were specified at the freestream conditions except for the streamwise velocity which had a turbulent boundary-layer profile described by the one-seventh power law. With such a velocity profile, the displacement and momentum thicknesses corresponding to a boundary-layer thickness of 0.003175 m (1/8 in.) are 0.002779 m and 0.0014801 m, respectively. The Reynolds number based on the displacement thickness at the inflow boundary was 59,000. Along segment B-C, postshock conditions based on inviscid, oblique shock-wave theory were specified. These postshock conditions were also specified along the freestream boundary (segment C-D). At the outflow boundary where the reflected shock wave exited the computational domain, the flow is also mostly supersonic except for a small region next to the wall so that all flow variables were extrapolated. Here, linear extrapolation based on three-point backward differencing was employed. The BCs imposed at the two side boundaries above the flat plate were the same as the ones imposed at the outflow boundary. At the exit of the plenum where the flow is subsonic, a back pressure P_b was imposed, and density and velocity were extrapolated in the same manner as the variables at the outflow boundary.

At all solid walls except for the two side walls of the plenum, the no-slip condition, adiabatic walls, and zero normal pressure gradient were imposed. At the two side walls of the plenum, the following inviscid BC was applied: the normal component of the velocity was set to zero; the first derivative of the tangential component of the velocity normal to the wall was taken to be zero; the wall was adiabatic; and the normal momentum equation was used to determine pressure. The inviscid BC was imposed at those walls because the boundary-layer flows next to them are assumed to affect inappreciably the bleed process due to their relatively large distance from the bleed hole. By treating those walls as inviscid, computational cost was reduced considerably by requiring less grid points next to those walls.

The initial conditions employed in this study were as follows. In the region above the flat plate, the initial condition was the two-dimensional steady-state solution for an incident and a reflected oblique shock wave on a flat plate based on inviscid, oblique, shock-wave theory. The streamwise velocity profile, however, was modified to give the one-seventh power law. To account for the change in mechanical energy within the boundary layer, the total energy per unit volume was modified as well. The initial conditions used in the bleed hole and plenum were stagnant air with density ρ_∞ at constant pressure P_b.

At this point it is important to note that the problem described in the preceding section appears to be symmetric about a plane that is perpendicular to the flat plate and passes through the middle of the inflow and outflow boundaries as well as the center of the bleed hole. This symmetry was not invoked in order to study the possibility of asymmetry that may result from vortex shedding downstream of the bleed hole, both above and below the flat plate.

Numerical Method of Solution

Solutions to the ensemble-averaged conservation equations of mass, momentum, and total energy closed by the Baldwin-Lomax algebraic turbulence model described in the preceding section were obtained by using the Overflow code developed at NASA Ames Research Center.[7] The Overflow code contains many algorithms. The one used in this study is as follows: All convection terms in the streamwise direction were upwind differenced by using the flux-vector splitting procedure of Steger and Warming.[8] All of the convection terms in directions normal to the streamwise direction were centrally differenced to reduce artificial dissipation

in those directions. All diffusion terms were also centrally differenced. The time-derivative terms were approximated by the Euler implicit formula. This low-order-accurate formula was used because previous studies[3–5] have shown that steady-state or quasi-steady-state solutions exist, and these are the ones sought here. The system of nonlinear equations that resulted from the aforementioned approximations to the space and time derivatives were analyzed by using the partially split method of Steger et al.[9] In Overflow, Jacobians and metric coefficients are interpreted as grid-cell volumes and grid-cell surface areas, respectively. In this regard, all algorithms in Overflow are implemented in the finite volume manner. However, BCs in Overflow are implemented in a finite-difference manner to enhance flexibility and ease in investigating different problems.

For the bleed-hole problem shown in Fig. 1, the computational domain was divided into three zones with three different coordinate systems to align upwind differencing with the streamwise direction. For this three-zone computational domain, a chimera grid system[10] with four overlapping grids was employed as shown in Figs. 2 and 3. Note that in those two figures the spatial dimensions were nondimensionalized by L (which is equal to 0.1778 m) as indicated by the coordinate system. The purpose of this coordinate system is to show the location in the computational domain where data is provided in the Results section.

For the zone above the flat plate, the grid system used was a single solution adapted H-H grid (adaptation was based on the initial conditions) which had grid points clustered near the flat plate, bleed hole, and the incident and reflected shock waves (Fig. 2). The number of grid lines used in this H-H grid were as follows: 155 grid lines from inflow to outflow, 101 grid lines from plate to freestream boundary, and 51 grid lines from side boundary to side boundary. The grid spacings in the direction normal to plate varied from 3.556 x 10^{-5} m at the plate to 3.556×10^{-3} m at the freestream boundary. The grid spacings in the streamwise direction varied from 7.112×10^{-3} m at the inflow boundary to 3.556×10^{-4} m at a distance of 0.019 m before where the incident shock wave would impinge on the plate under inviscid conditions. From 0.019 m before the inviscid-shock-impingement point to 0.019 m after that point, the grid spacings in the streamwise direction were kept constant at 3.556×10^{-4} m. From 0.019 m after the shock-impingement point to the outflow boundary, the grid spacings varied from 3.556×10^{-4} m to 5.334×10^{-3} m.

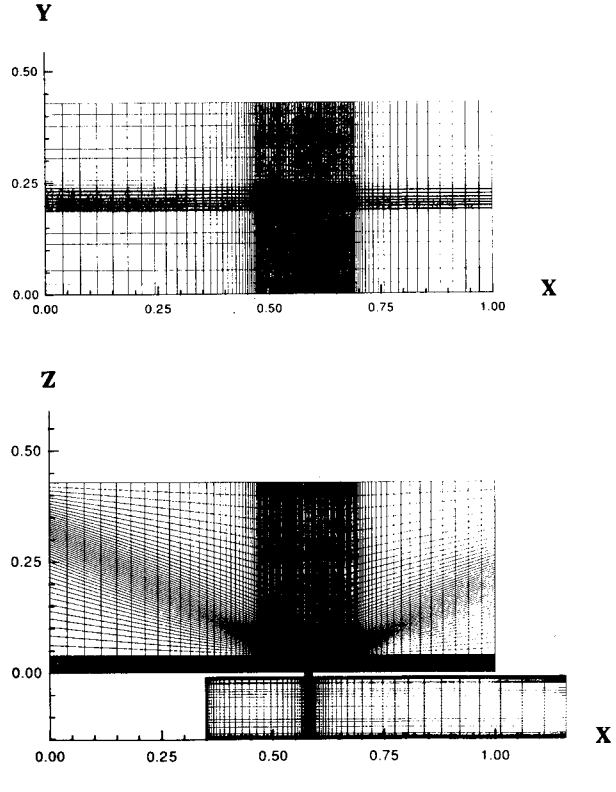

Fig. 2 Grid system used.

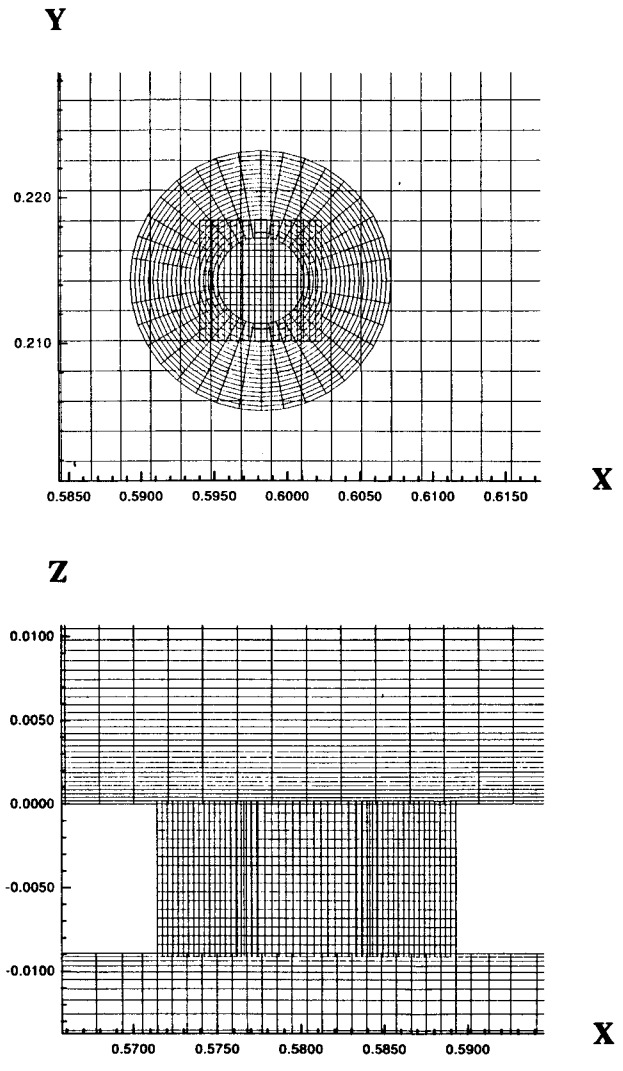

Fig. 3 Grid system in the region about the bleed hole.

For the zone containing the bleed hole, two overlapping grids were used: an O-H grid touching the wall of the bleed hole and an H-H grid at the center of the bleed hole (Fig. 3). The O-H grid with $20\times37\times21$ grid points was used to resolve the circular geometry of the bleed hole. The H-H grid with $20\times21\times21$ grid points was used to eliminate the centerline singularity associated with the O-H grid. For the zone containing the plenum, a single H-H grid was used (Fig. 2). This H-H grid had $81\times51\times50$ grid points with grid points clustered near walls and the bleed hole. Note that grid spacings in different grids were made comparable in regions where they overlapped to minimize aliasing errors (Fig. 3).

The grid system just described was generated by using algebraic grid generation with Vinokur's one-dimensional stretching functions.[11] The clustering and the number of grid points employed were arrived at after considerable numerical experiments to ensure the following. First, the grid must be able to discern effects that result from moving the bleed hole by only 0.003175 m (1/8 in.). This required crisp resolution of the incident and reflected shock waves. Second, qualitative features of the predicted flowfield must be grid independent. Only the qualitative features were used to construct a model for the underlying physics of shock-wave/boundary-layer interactions with bleed since the turbulence model used is suspect.

During computations, the flowfield in each grid was analyzed one at a time in the following order: the H-H grid above the flat

plate, the H-H grid in the bleed hole, the O-H grid in the bleed hole, and the H-H grid in the plenum. Information from one grid was passed to another grid via trilinear interpolation at grid boundaries. The required interpolation coefficients were obtained by using the Pegasus code.[11] This process of analyzing the flow in one grid at a time until all of the grids are analyzed was repeated for each time step until a converged solution was obtained. Here, a solution is assumed to be converged if the second norm of the residual leveled out for at least 500 time steps. Typically, at that time, the second norm was about 10^{-7}. Here, it is noted that the residual oscillated about some average value as it leveled out, and the amplitude of those oscillations were less than 10^{-7} when the residual was 10^{-7}.

At this point, it is important to note that three bleed-hole locations and one shock-impingement point were used instead of three shock-impingement points and one bleed-hole location. The reason for moving the bleed hole instead of the shock generator was to ensure that the computed flowfield above the flat plate would be the same whether the bleed hole was at, before, or after the incident shock when bleeding had not started. This criterion is important because it establishes a common reference about which comparisons can be made. It turns out that if the shock-impingement point moved instead of the bleed-hole location, then this criterion cannot be satisfied if nonuniform grids are used and if the dissipative nature of the numerical scheme is anisotropic.

Results

Numerical solutions were obtained to investigate the physics of three dimensional, shock-wave/boundary-layer interactions with bleed for the problem described and formulated in the preceding sections and depicted in Fig. 1. Three different bleed-hole locations relative to the "inviscid" shock-wave impingement point were studied; namely, bleed hole at, before, and after the incident shock. The results of this study are given in Figs. 4–11. Before describing these results in detail, note that Figs. 4–7 show the Mach number contours; Fig. 8 shows the pressure contours; Figs. 9 and 10 show the pressure distribution on the wall; and Fig. 11 shows the distribution of the absolute vorticity on the wall. Also, note that the results for the Mach number and pressure are given along three planes, seen from the side, top, and back. For the side and back views, the planes pass through the center of the bleed hole. For the top view, the plane is parallel to the flat plate but 0.0001544 m (0.00608 in.) above it. For each figure, a coordinate system is attached which shows its relative size and location in the domain.

The results contained in the aforementioned figures are presented in the following order. First, they are used to reveal the underlying mechanism by which bleed holes control shock-wave/boundary-layer interactions. Afterward, they are used to describe the effects of bleed-hole placement on upstream, spanwise, and downstream influence lengths.

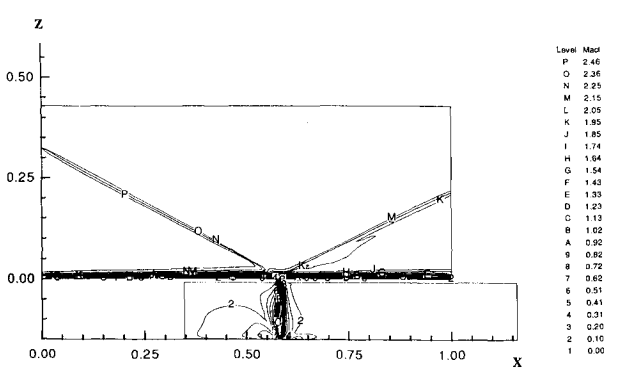

Fig. 4 Mach number contours for the case in which bleed hole is at inviscid shock-impingement point (side view).

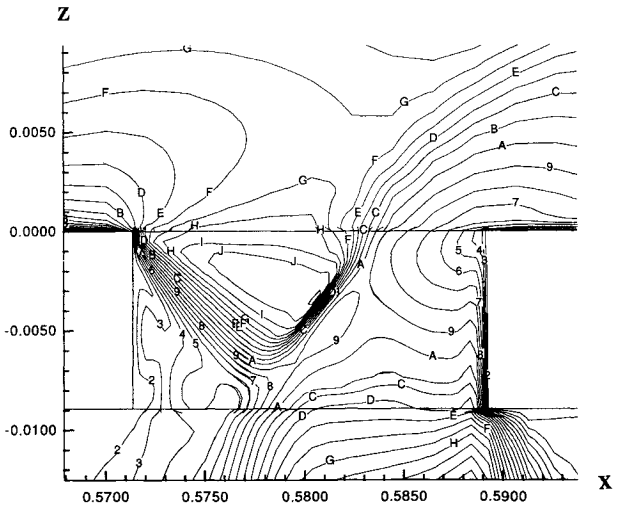

Fig. 5 Mach number contours near bleed hole for the case shown in Fig. 4 (side view); contour definitions same as those given in Fig. 4.

Physics of Shock-Wave/Boundary-Layer Interactions with Bleed

It is well known (e.g., see Ref. 1) that when a shock wave impinges on a boundary layer (BL) terminating at the sonic line, the displacement thickness of the BL upstream of the impingement point increases. This is because the adverse pressure gradient created by the incident shock propagates upstream through the subsonic portion of the BL. The thickened BL upstream of the impingement point in turn causes the approaching supersonic flow to form compression waves which coalesce into a reflected shock wave. The adverse pressure gradient created by the incident shock, if sufficiently strong, can induce flow separation. The purpose of bleed is to control this shock-wave induced flow separation. How bleed accomplishes this task for supersonic flow with shock waves has not been well understood.

In this study, two mechanisms are proposed by which bleed can control shock-wave/boundary-layer interactions. Both mechanisms proposed hinge on the fact that a shock is created by the bleed process. First, the formation of this shock is identified and explained. Afterward, its properties are examined. Finally, how this shock can be utilized to control shock-wave/boundary-layer interactions is described.

Formation of a Shock by Bleed

From Figs. 5, 7, and 8, one can readily see that a shock forms in and around the downstream edge of the bleed hole when there is bleed. A schematic diagram of this shock is shown in Fig. 12. With the shock identified, let us examine why and how it forms. When the flow is supersonic, bleeding of the subsonic portion of the BL causes the streamline separating the subsonic from the supersonic part to bend downward toward the flat plate and bleed hole. This is illustrated in Fig. 12, and can be deduced from Figs. 5 and 8. The downward bending of that streamline causes the supersonic part of the BL to undergo Prandtl-Meyer expansion which accelerates it. When the accelerated supersonic portion of the BL approaches the bleed hole, a shock forms due to the compression-corner effect because the flow must change direction, either into the bleed hole or along the flat plate (see Fig. 12). Thus, the shock formed is a two-segment shock system: one segment inside the bleed hole (created by the supersonic flow that turned into the bleed hole) and the other segment toward the downstream edge of the bleed hole and extending above the plate (created by the supersonic flow that did not enter the bleed hole but turned to flow along the plate).

At this point, note that the two-segment shock system just mentioned could be either attached oblique shocks as shown in Fig. 12 or a detached bow shock as shown in Figs. 5 and 8. The bow shock would form if the turning angles α_1 and α_2 were sufficiently large, which is the case for the present study with β equal to 90 deg (see

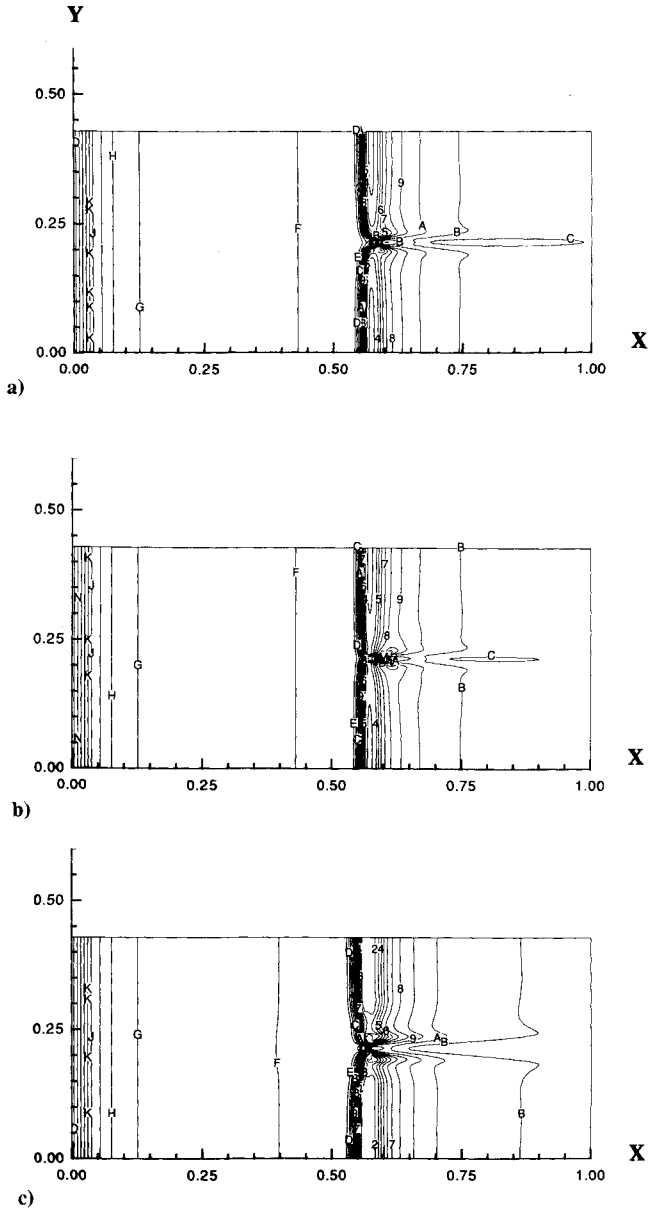

Fig. 6 Mach number contours (top view): a) bleed hole at shock; b) bleed hole after shock; and c) bleed hole before shock. Contour definitions same as those given in Fig. 4.

Fig. 12). Conversely, if these turning angles are zero, then no oblique shocks would form.

Properties of that Shock

One important property of the two-segment shock system is that the pressure rise across it can be higher than that created by the incident shock (see Fig. 9). There are two reasons for this. First, the Mach number of the flow creating the two-segment shock system can be higher than the freestream Mach number (recall that the flow underwent Prandtl-Meyer expansion). Second, the "turning" angle required of the supersonic flow can be higher (see α_1 and α_2 in Fig. 12). Both of these affects lead to a stronger shock.

Another important property of the two-segment shock system is that it increases mixing in directions normal to the streamwise direction in the region above the flat plate and just downstream of the bleed hole. This is because the top part of the two-segment shock system dramatically disrupts the flow there. This disruption is a result of the interactions between two streams of supersonic flow, one that passed through the top part of the two-segment shock system and the other that went around it. The stream that passed through the shock had its speed lowered and its static pressure increased. But, for the stream that went around the shock instead of through it, its speed and static pressure remained essentially unchanged. When these two streams meet just downstream of the top part of the two-segment shock system, very significant gradients in pressure and velocity form. The pressure gradient can create blast waves, whereas the velocity gradient can create highly turbulent shear layers. Both of these phenomena would greatly enhance mixing. In this regard, the two-segment shock system behaves like turbulence and blast-wave generators.

Mechanisms Made Possible by Shock

The two properties mentioned for the two-segment shock system can be used to construct mechanisms to explain how bleed hole or holes control shock-wave/boundary-layer interactions. Here, two mechanisms are proposed. The first mechanism is based on the realization that the pressure rise across the the two-segment shock system can be higher than the one produced by the incident shock (i.e., the two-segment shock system about the bleed hole can be stronger than the incident shock). If this is the case, then the two-segment shock system can serve as a barrier, preventing any information downstream of it from propagating upstream. Henceforth, if a two-segment shock system is stronger than the incident shock, it will be referred to as a barrier shock.

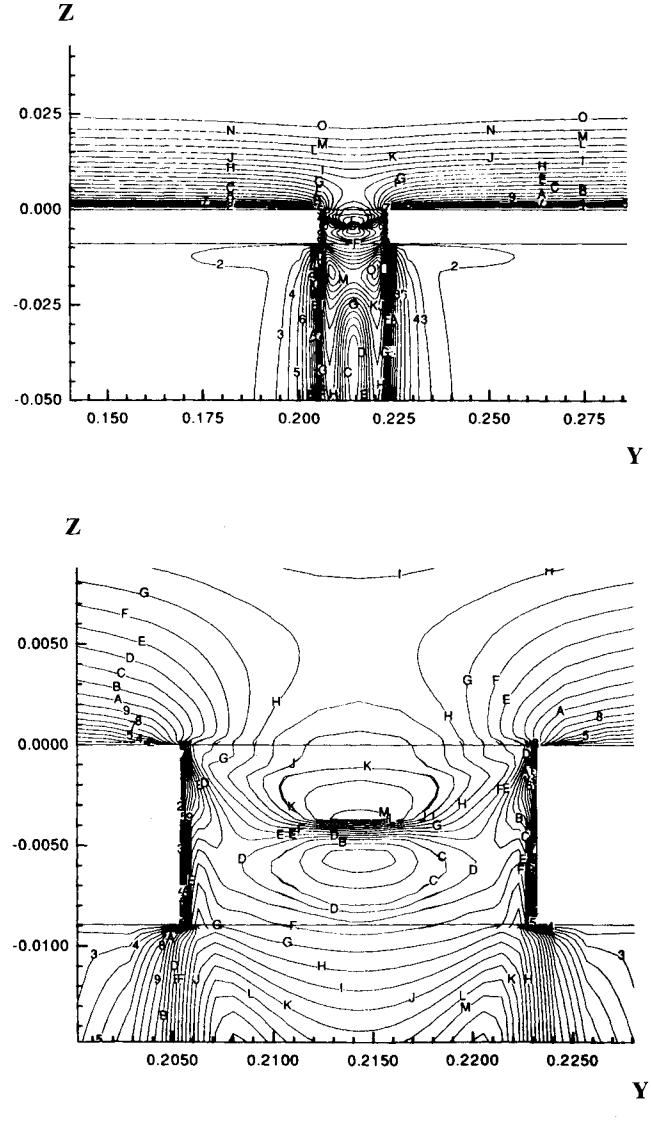

Fig. 7 Mach number contours near bleed hole for the case shown in Fig. 4 (back view); contour definition: all levels are equally incremented by 0.0917 so that the levels 1, 2,..., 9, A, B,..., P denote 0.00, 0.09,..., 0.73, 0.83, 0.92,..., 2.20, respectively.

Since the barrier shock is always located in and toward the downstream edge of the bleed hole, its effectiveness depends on the location of the bleed hole. Thus, when placing a bleed hole, one should place it slightly before the location where the incident shock impinges on the sonic line of the BL so that the barrier shock is formed upstream of any disturbances created by the incident shock. If the bleed hole is placed after where the incident shock impinges on the BL, then the blocking capability of the barrier shock is not put to full use (see Fig. 8). Note that the adverse pressure gradient created by the barrier shock does not cause flow separation. This is because only supersonic flow enters the two segments of that shock, and boundary-layer formation takes place after the shock where the pressure has already been elevated.

The second mechanism by which bleed hole or holes affect shock-wave/boundary-layer interactions is the fact that the top part of the two-segment shock system can behave like turbulence and blast-wave generators (see the second property of the two-segment shock system mentioned earlier). Turbulence and blast-wave generators can greatly enhance mixing. The blast wave also induces a velocity in the spanwise direction. This increased mixing and the induced spanwise velocity can affect shock-wave/boundary-layer interactions in two ways. First, it increases the momentum of the fluid near the wall, and this enables the BL to resist higher pressure gradients without separating. Second, it can be utilized to control nonuniformities in the boundary-layer profile and distortions in the flow downstream of the incident shock.

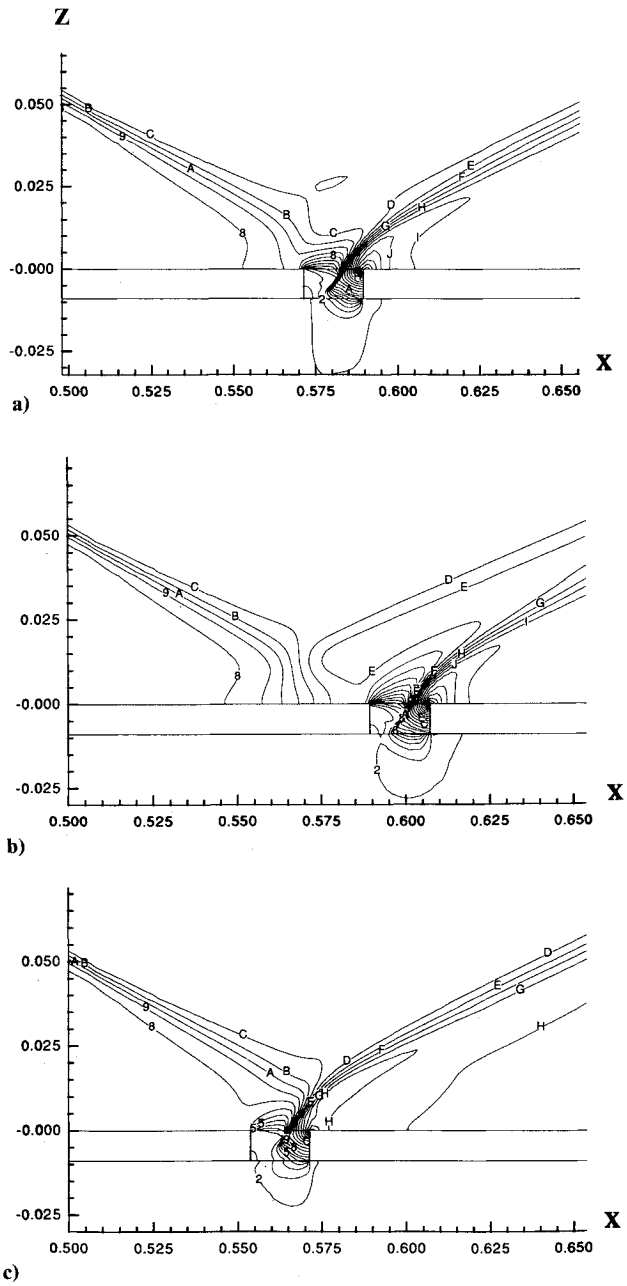

Fig. 8 Pressure contours near bleed hole (side view); a) bleed hole at shock, b) bleed hole after shock, and c) bleed hole before shock. Contour definition: all levels are equally incremented by 1.315×10^3 Pa so that the levels 1, 2,..., 9, A, B,..., P denote 1.42, 2.74,..., 12.0, 13.3, 14.6,..., 33.0×10^3 Pa, respectively.

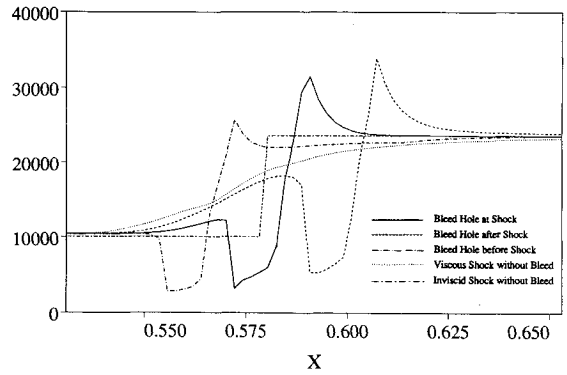

Fig. 9 Pressure along wall from inflow to outflow passing through center of bleed hole.

Several consequences of the mechanisms just proposed are as follows. First, if a bleed hole is slanted (e.g., if β in Fig. 12 is less than 90 deg, say 45 deg), then the turning angle of the supersonic flow into the bleed hole may be such that no shock forms inside the bleed hole. For this case, the turning angle of the supersonic flow along the flat plate is also less, so that only a weak oblique shock forms on the downstream edge of the bleed hole on the plate. However, since the flow is supersonic at the downstream edge of the bleed hole and the subsonic portion of the BL is just beginning to form there (i.e., the downstream edge of the bleed hole is the leading edge of the supersonic BL), again no disturbances can propagate upstream of the bleed hole. Second, if P_b is sufficiently low and β in Fig. 12 is equal to 90 deg, then when there are multiple holes, every bleed hole would have a barrier shock. These barrier shocks can create considerable disturbances in the flow, much like a rough surface.

At this point, note that the physics just described would take place regardless of the turbulence model used. This is because turbulence only effects the degree of mixing and not whether shocks and blast waves form or not, although the unsteadiness due to eddying motion can affect shock structure by making them oscillate about some mean (magnitude and position). In this study, only shocks, blast waves, and their formation were utilized in devising the underlying mechanisms of the bleed process. Since shocks and their location are important to the conclusions of this study, note the sharpness with which the incident and reflected shocks were resolved by the solution-adapted grid (see Figs. 4 and 8).

Effects of Bleed-Hole Placement

With two mechanisms by which bleed holes control shock-wave/boundary-layer interactions described, those mechanisms are now used to explain the predicted upstream, spanwise, and downstream influence lengths as a function of bleed-hole placement in relation to where the incident shock impinged on the sonic line of the BL.

Upstream Influence Length

Figure 9 shows the pressure distribution on the wall for the following cases: inviscid wall, viscous wall with no bleed, and viscous wall with bleed (bleed hole at, before, and after the inviscid shock-impingement point). According to this figure, when there is bleed, the upstream influence length is reduced when compared to

the case with no bleed. However, the reduction is greatest when the bleed hole is located slightly before the incident shock. In fact, for this case, there was no adverse pressure gradient before the bleed hole, indicating that the barrier shock was able to eliminate completely the upstream influence length under the conditions of the present study. When the bleed hole is located at or after the shock, there were adverse pressure gradients before the bleed hole. This is because the barrier shock was set up too far downstream so that some of the effects of the incident shock have already propagated upstream (see Fig. 8). At this point, it should be noted that the incident shock bends inward as it enters the supersonic part of the BL.[1] Thus, the bleed hole that is located at the inviscid shock-impingement point is really located slightly downstream of where the incident shock actually impinged on the sonic line of the BL.

The question now is whether separation can be eliminated by the bleed process? To answer this question, see the absolute value of the vorticity along the wall given in Fig. 11. When there is separation, vorticity goes to zero. From Fig. 11, it can be seen that when there is no bleed, the flow separates at X near 0.565 and reattaches at X near 0.585. When there is bleed, whether the bleed hole is at, before, or after the incident shock, Fig. 11 shows that flow separation does not take place. However, for a stronger incident shock, separation can still occur since adverse pressure gradients existed when the bleed hole was placed at and after the incident shock (see Fig. 9). Only when the bleed hole is placed slightly before the incident shock was there no adverse pressure gradients. Thus, it is important to place bleed holes judiciously.

Spanwise Influence Length

The spanwise influence length can be inferred by examining Figs. 6, 7, and 10. From these figures, it can be seen that the spanwise influence length is the greatest when the bleed hole is located upstream of the incident shock and the smallest when the bleed hole is located downstream of it. One reason for this is that when

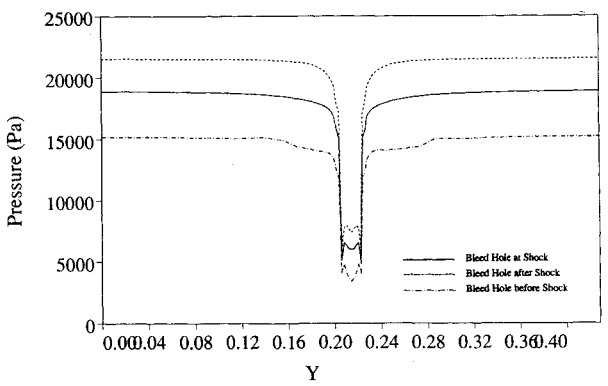

Fig. 10 Pressure along wall from side boundary to side boundary passing through center of bleed hole.

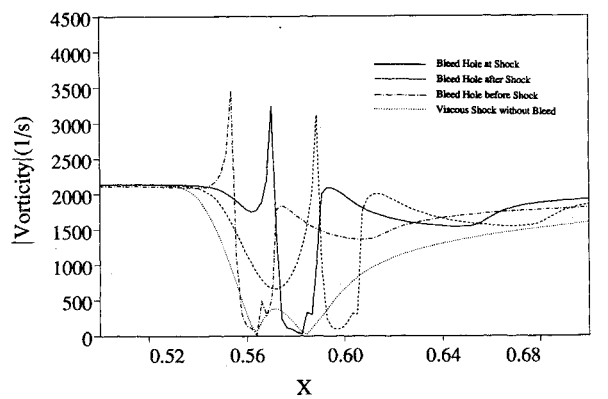

Fig. 11 Absolute vorticity along wall from inflow to outflow passing through center of bleed hole.

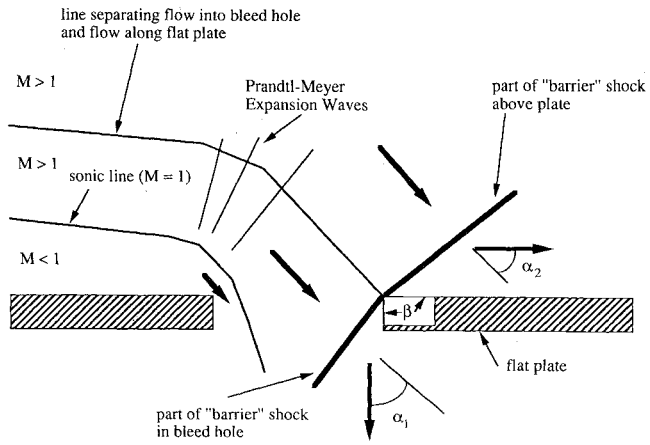

Fig. 12 Schematic diagram of the two-segment shock system (barrier shock) about a bleed hole; if the turning angles α_1 and α_1 are sufficiently large, then the oblique shock waves shown can detach as shown in Figs. 5 and 8.

the bleed hole is located upstream of the incident shock, the ratio of the pressure just downstream of the barrier shock to the pressure of the fluid that flows around it is the highest. This is because the fluid that flows around the barrier shock has not yet been elevated by the incident shock. This pressure ratio can cause blast waves and flow in the spanwise direction.

The spanwise influence length is important when bleed holes are to be placed side by side. At this point, note that the flow is symmetric in the spanwise direction about the plane that passes through the center of the bleed hole (see Figs. 6, 7, and 10). Recall that this symmetry was not enforced in the computations, although efforts were not made to ensure the resolution of all spatial and temporal disturbances that may be needed to trigger the asymmetry.

Downstream Influence Length

The downstream influence length can be inferred from Fig. 6. This figure shows that the bleed hole can create a very large wake in the Mach number (the wake in pressure is somewhat smaller and is not shown). Further examination of Fig. 6 shows that the wake in Mach number is the largest when the bleed hole is before the shock. The reason for this is the same as the one presented for the spanwise influence length.

Summary

A numerical study was conducted to investigate the physics of three-dimensional, shock-wave/boundary-layer interactions on a flat plate with bleed through a circular hole connected to a plenum. This study identified and explained the reason for the formation of a two-segment shock system, referred to as the barrier shock. Based on the barrier shock, two mechanisms were proposed by which bleed holes can control the response of a boundary layer to incident shock waves. This study also showed how bleed-hole placement in relation to shock-wave impingement effects upstream, spanwise, and downstream influence lengths. Currently, efforts are underway to study the effects of multiple bleed holes (staggered and nonstaggered arrangements), different plenum back pressures P_b, and different boundary-layer profiles on shock-wave/boundary-layer interactions with bleed.

Acknowledgment

This research was supported by NASA Grant NAG 2-709. All computations were obtained on a Cray-2 computer at the NAS facility.

References

[1]Delery, J. M., "Shock Wave / Turbulent Boundary Layer Interaction and Its Control," *Progress in Aerospace Sciences*, Vol. 22, 1985, pp. 209–280.

[2]Hamed, A., and Shang, J., "Survey and Assessment of the Validation

Data Base for Shock Wave Boundary Layer Interactions in Supersonic Inlets," *Journal of Propulsion and Power,* Vol. 7, No. 4, 1991, pp. 617–625.

[3]Hamed, A., and Lehnig, T., "An Investigation of Oblique Shock/Boundary Layer/Bleed Interaction," *Journal of Propulsion and Power,* Vol. 8, No. 2, 1992, pp. 418–424.

[4]Hamed, A., and Lehnig, T., "The Effect of Bleed Configuration on Shock/Boundary Layer Interactions," AIAA Paper 91-2014, June 1991.

[5]Hahn, T. O., Shih, T. I-P., and Chyu, W. J., "Numerical Study of Shock-Wave/Boundary-Layer Interactions with Bleed," *AIAA Journal,* Vol. 31, No. 5, 1993, pp. 869–876.

[6]Baldwin, B., and Lomax, H., "Thin Layer Approximation and Algebraic Model for Separated Turbulent Flows," AIAA Paper 78-257, Jan. 1978.

[7]Buning, P. G., and Chan, W. M., "OVERFLOW/F3D User's Manual," NASA Ames Research Center, unpublished, March 1991.

[8]Steger, J. L., and Warming, R. F., "Flux-Vector Splitting of the Inviscid Gasdynamic Equations with Application to Finite-Difference Methods," *Journal of Computational Physics,* Vol. 40, No. 2, 1981, pp. 263–293.

[9]Steger, J. L., Ying, S. X., and Schiff, L. B., "A Partially Flux-Split Algorithm for Numerical Simulation of Compressible Inviscid and Viscous Flow," *Proceedings of the Workshop on Computational Fluid Dynamics,* Institute of Nonlinear Sciences, University of California, Davis, CA, 1986.

[10]Benek, J. A., Buning, P. G., and Steger, J. L., "A 3-D Chimera Grid Embedding Technique," AIAA Paper 85-1523, July 1985.

[11]Vinokur, M., "On One-Dimensional Stretching Functions for Finite-Difference Calculations," *Journal of Computational Physics,* Vol. 50, No. 1, 1983, pp. 215–234.